Hindawi
Mathematical Problems in Engineering
Volume 2019, Article ID 3182736, 10 pages
https://doi.org/10.1155/2019/3182736

Research Article

Novel Intelligent Approach for Peak Shear Strength Assessment of Rock Joints on the Basis of the Relevance Vector Machine

Caichu Xia,[1,2] **Man Huang**,[1,2] **Xin Qian**,[1] **Chenjie Hong**,[2] **Zhanyou Luo**,[3] **and Shigui Du**[2]

[1]*Department of Geotechnical Engineering, Tongji University, 1239 Siping Road, Shanghai 200092, China*
[2]*Department of Civil Engineering, Shaoxing University, 508 Huancheng West Road, Shaoxing 312000, Zhejiang, China*
[3]*Geotechnical Engineering Institute, Zhejiang University of Science and Technology, 318 Liuhe Road, Hangzhou 310023, Zhejiang, China*

Correspondence should be addressed to Man Huang; hmcadx@126.com

Received 13 July 2019; Accepted 30 November 2019; Published 19 December 2019

Academic Editor: Luis Cea

Copyright © 2019 Caichu Xia et al. This is an open access article distributed under the Creative Commons Attribution License, which permits unrestricted use, distribution, and reproduction in any medium, provided the original work is properly cited.

This study mainly establishes a novel intelligent assessment model for peak shear strength of rock joints based on the relevance vector machine (RVM). RVM is a state-of-the-art soft computing technique that has been rarely utilized in joint shear strength assessment. To establish the hybrid intelligent model, three-dimensional scanning tests and direct shear tests on 36 granite joint specimens were conducted. The peak shear strength ratio (τ_p/σ_n) is perceived as an explanation of four types of influencing factors, including joint surface roughness, strength of rock material, basic friction angle, and normal stress. In particular, the compressive strength and tensile strength of rock material are first considered together. A total of 36 experimental data were used in this study to train the RVM model to predict the peak shear strength of rock joints. The performance of the RVM model was assessed using the direct shear test data of rock joints collected from previous researches. Four different kinds of kernel functions were adopted to obtain the optimal model. Results show that the proposed model is significantly efficient in predicting the peak shear strength of rock joints. The proposed model is also a promising tool for peak shear strength of rock joints and provides a new research approach to research the mechanical properties of rock joints.

1. Introduction

The deformation capacity, strength, and stability of fractured rock mass are strongly influenced by the shear behavior of joints. Therefore, the accurate determination of shear strength is the key to design the safety structure in rock mass or rock masses [1]. Over the past decades, empirical [2–9], semi-theoretical [10], and theoretical methods [11] have been proposed to determine the shear strength of rock joints. Various factors, such as rock type, joint surface roughness, joint size, and infilling materials, exhibit a wide variation of joint shear strength [12, 13]. Considering their strong randomness, fuzziness, and uncertainty, the peak shear strength of rock joints has a complex nonlinear relationship with the aforementioned factors [14, 15]. The traditional methods demonstrate strong usability and dependability in practical engineering, but large computations and complex algorithms limit the use of these methods. Thus, the deterministic analysis methods in assessing the joint shear strength remain difficult. In recent years, data mining and artificial intelligence technologies, such as artificial neural network (ANN) and support vector machine (SVM), have been widely used to estimate the mechanical properties of rocks, such as the compressive strength and tensile strength [16–21]. However, ANN has several disadvantages, such as poor generalizing performance, large training data requirement, slow convergence velocity, and over-fitting problem [22–24]. SVM can effectively solve the aforementioned problems and exhibit excellent generalization capability and high regression accuracy [25, 26]. Despite many advantages, SVM suffers from several limitations. The output of an SVM represents decisions rather than posterior

probabilities [27]. In addition, the kernel function of SVM must fulfill Mercer's condition. The relevance vector machine (RVM) is a probabilistic model based on Bayesian theory for regression and classification; it has high generalization capability, sparse model structure, and low computation complexity, avoiding the principal limitations of SVM [28]. Especially for small samples, RVM can map the limited input data into a high-dimensional feature space and finally use several relevance vectors to deal with the dimensionality problems. The primary purpose of this study is to introduce a reliable estimation method of peak shear strength of rock joints on the basis of RVM. To this end, 36 rock joints under different stress were designed and tested in laboratory. The rest of this article is organized as follows: Section 2 presents the theoretical background of RVM. Section 3 introduces the description of the experimental procedure and results. Section 4 describes the establishment of the RVM model. Section 5 presents the comparison and discussion. The final section presents the conclusions.

2. RVM Method

RVM is a probabilistic learning model based on the Bayesian framework to solve complex regression and classification problems [28]. It generates a mapping between the targets $\{t_n\}_{n=1}^N$ and the corresponding input vectors $\{x_n\}_{n=1}^N$.

$$t_n = y(x_n;\omega) + \varepsilon_n = \sum_{n=1}^{N} \omega_n K(x, x_n) + \omega_0 + \varepsilon_n, \tag{1}$$

where N is the total sample number, n is the nth sample number, y is the output variable, ω_n is the weight of the nth sample, $K(x, x_n)$ is the kernel functions, and ε_n is a mean-zero white noise process with variance σ^2.

Assuming an independent distribution for t_n, the likelihood of the entire dataset can be expressed as follows:

$$p\left(\mathbf{t} \mid \boldsymbol{\omega}, \sigma^2\right) = \left(2\pi\sigma^2\right)^{-N/2} \exp\left(-\frac{\|\mathbf{t} - \boldsymbol{\Phi}\boldsymbol{\omega}\|^2}{2\sigma^2}\right), \tag{2}$$

where $\mathbf{t} = \{t_1, t_2, \ldots, t_N\}^{\mathrm{T}}$, $\boldsymbol{\omega} = \{\omega_0, \omega_1, \ldots, \omega_N\}^{\mathrm{T}}$, and $\boldsymbol{\Phi}(x_n) = \{1, K(x_n, x_1), \ldots, K(x_n, x_N)\}^{\mathrm{T}}$.

Direct maximum-likelihood estimation of ω from equation (2) may suffer from overfitting [29]. Therefore, a zero-mean Gaussian prior distribution over every weight ω_i with the diagonal covariance α is adopted and described as follows:

$$p(\omega \mid \alpha) = \prod_{i=0}^{N} N\left(\omega_i \mid 0, \alpha_i^{-1}\right). \tag{3}$$

The posterior distribution for the weights can then be calculated using Bayes' law based on the Gamma prior distributions [30]:

$$p\left(\omega \mid t, \alpha, \sigma^2\right) = \frac{p\left(t \mid \omega, \sigma^2\right) p(\omega \mid \alpha)}{p(t \mid \alpha, \sigma^2)}. \tag{4}$$

Integrating the weight parameters, the marginal distribution of hyperparameters α and σ^2 can be obtained:

$$p\left(t \mid \alpha, \sigma^2\right) = (2\pi)^{-N/2} |\Omega| \exp\left(\frac{-t^{\mathrm{T}}\Omega^{-1}t}{2}\right), \tag{5}$$

where $\Omega = \sigma^2 E + \Phi A^{-1}\Phi^{\mathrm{T}}$, $A = \mathrm{diag}(\alpha_0, \alpha_1, \ldots, \alpha_N)$, and E is a unit vector. Taking its partial derivatives to equation (5) by iteration, the values of α and σ^2 can be obtained.

3. Experimental Procedure and Results

3.1. Preparation of Rock Samples. To investigate the effect of wide-range normal stress on peak shear strength, rectangular granite joints were selected for the direct shear tests because of their high strength. Rectangular blocks of rock specimens with dimension of 100 mm × 100 mm × 200 mm were labeled as SJ1–SJ36. Brazilian splitting tests were conducted by using a TSF-600 shear-flow coupled test system for rock joints at Tongji University. The granite joint surface dimensions were approximately 100 mm wide and 200 mm long (Figure 1). After testing, no apparent defects were found in the specimens. σ_c is the uniaxial compressive strength, σ_t is the tensile strength, E is Young's modulus, ρ is the rock density, and γ is Poisson's ratio, and basic friction angle φ_b was determined using the suggested methods of the International Society for Rock Mechanics (ISRM) [31], and the results are listed in Table 1.

3.2. Surface Topography Measurement. To investigate the influence of the three-dimensional (3D) surface roughness on the mechanical properties of rock joints quantitatively, the joint surface topography of measuring each shear test sample block before using a noncontact direct shear test, 3D stereo-topometric measurement system (positioning accuracy: 20 μm) was developed by Xia et al. [32]. Before the estimation of joint surface roughness, the 3D surface topography was reconstructed on the basis of the interpolation of the scanned point clouds. Tatone and Grasselli indicated that the digitized surface topographies of rock joints with sampling interval <0.55 mm using linear interpolation technique can capture microfeatures of surface morphology [33]. In this study, we set the sampling intervals in length (L) and width (W) directions to be 0.3 mm. Taking upper surface topographies of four joint samples as examples, the digitized surface topographies of rock joints (the height magnified to 3 times its normal size) are shown in Figure 2.

3.3. Test Procedure and Results. This test was designed to obtain an extensive peak shear strength model of rock joints. We conduct the direct shear tests on the test samples under nine normal stress levels, namely, 1.0, 2.0, 3.0, 5.0, 8.0, 10.0, 12.0, 15.0, and 20.0 MPa. Four direct tests were performed on the test specimen at each level of normal stress. The values of the peak shear strength for each test specimen are listed in Table 2. The rate of shear displacement was set to be 0.5 mm/min, and the maximum displacement was 20 mm which is 10% of the joint length.

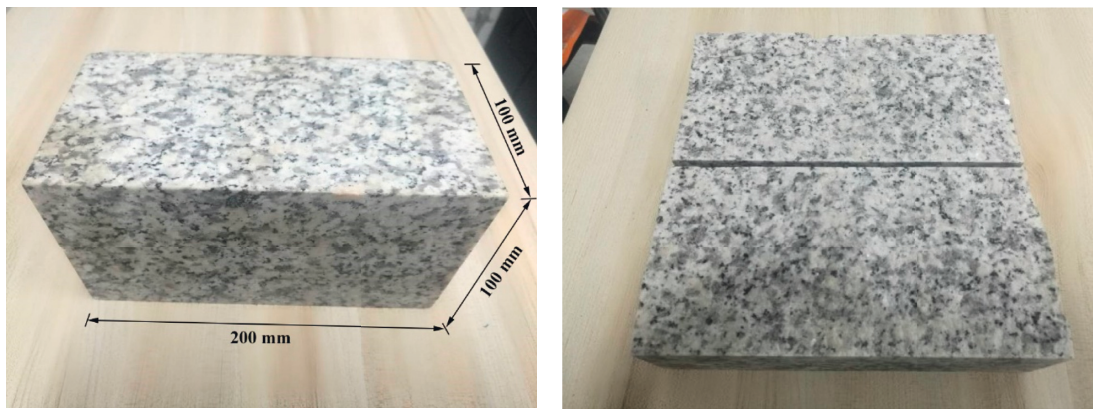

(a) (b)

Figure 1: Granite block and granite joint specimen.

Table 1: Physical and mechanical parameters of granite rock.

σ_c (MPa)	σ_t (MPa)	E (GPa)	P (g/cm^3)	γ	φ_b
161.0	10.8	45.5	2.64	0.23	33.28°

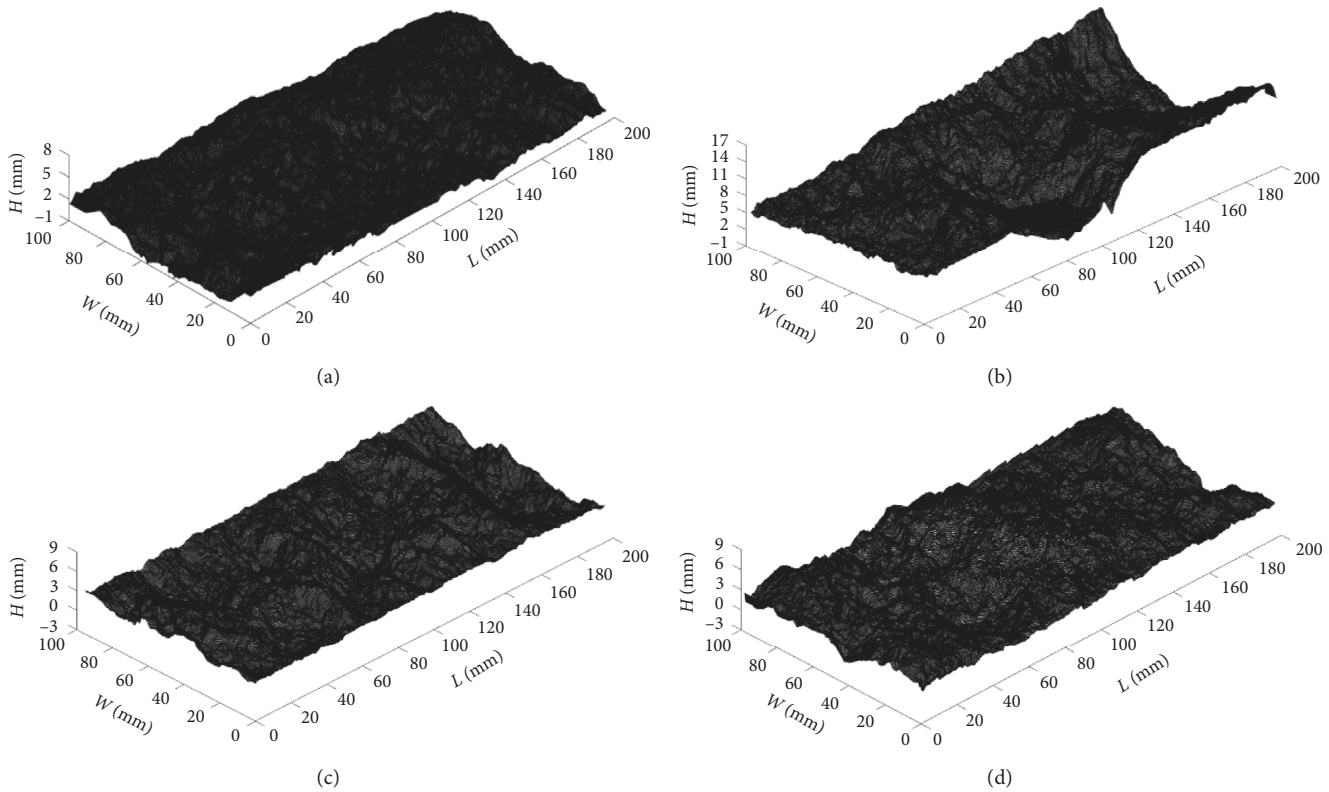

Figure 2: 3D digitized upper surface topographies of rock joints: (a) SJ3, (b) SJ12, (c) SJ21, and (d) SJ30.

4. Establishment of a Peak Shear Strength Assessment Model Based on RVM

4.1. Selecting the Influencing Factors. According to the study by Barton and Choubey [34], the joint surface roughness, rock material strength, basic friction angle, and normal stress exhibit a wide variation of shear behavior. Therefore, normal stress, joint surface roughness, rock strength, and basic friction angle were selected in this work to assess the peak shear strength.

Various parameters, including empirical, statistical, and fractal, have been proposed to quantify the surface roughness of rock joints. Numerous experimental tests demonstrated that partial contact between the lower and upper joint surface was located in the steepest zones facing the

Table 2: Peak shear strength of test specimens.

Sample name	σ_n (MPa)	τ_p (MPa)
SJ1	1	2.30
SJ2	2	4.55
SJ3	3	4.78
SJ4	5	8.30
SJ5	8	9.63
SJ6	10	12.75
SJ7	12	13.64
SJ8	15	17.28
SJ9	20	21.26
SJ10	1	1.89
SJ11	2	3.64
SJ12	3	7.41
SJ13	5	8.28
SJ14	8	11.15
SJ15	10	13.23
SJ16	12	14.61
SJ17	15	18.07
SJ18	20	19.76
SJ19	1	3.07
SJ20	2	3.65
SJ21	3	5.46
SJ22	5	7.05
SJ23	8	11.92
SJ24	10	12.57
SJ25	12	14.49
SJ26	15	16.15
SJ27	20	20.99
SJ28	1	2.49
SJ29	2	5.21
SJ30	3	5.29
SJ31	5	7.70
SJ32	8	13.18
SJ33	10	12.23
SJ34	12	15.44
SJ35	15	17.74
SJ36	20	24.91

Table 3: 3D morphology parameters of test specimens.

Sample name	A_0	$\theta^*_{max}/(C+1)$ (deg)
SJ1	0.479	10.465
SJ2	0.498	12.433
SJ3	0.504	10.139
SJ4	0.510	12.384
SJ5	0.467	10.870
SJ6	0.477	12.718
SJ7	0.542	10.237
SJ8	0.504	10.197
SJ9	0.472	10.208
SJ10	0.502	9.952
SJ11	0.484	11.961
SJ12	0.498	14.253
SJ13	0.528	14.405
SJ14	0.520	11.266
SJ15	0.498	10.411
SJ16	0.508	10.659
SJ17	0.501	11.699
SJ18	0.485	11.298
SJ19	0.496	12.499
SJ20	0.481	10.708
SJ21	0.505	12.808
SJ22	0.532	12.134
SJ23	0.471	14.002
SJ24	0.505	11.191
SJ25	0.499	11.398
SJ26	0.495	10.365
SJ27	0.433	10.083
SJ28	0.493	11.231
SJ29	0.498	13.550
SJ30	0.501	10.829
SJ31	0.512	11.177
SJ32	0.502	11.975
SJ33	0.454	10.467
SJ34	0.479	12.858
SJ35	0.492	9.942
SJ36	0.514	15.303

shear direction during the shearing [35–37]. Grasselli et al. [38] established a relationship between total potential contact area ratio A_{θ^*} and the corresponding apparent dip angle θ^*, as shown in the following equation:

$$A_{\theta^*} = A_0 \left[\frac{\theta^*_{max} - \theta^*}{\theta^*_{max}} \right]^C, \quad (6)$$

where A_0 is the maximum potential contact area under apparent dip angle θ^* at 0°; θ^*_{max} is the maximum apparent dip angle in the shear direction; and C is a dimensionless roughness parameter characterizing the distribution of the apparent dip angle over the surface, which is calculated using equation (6). Considering the possible range of $C \in (0, \infty)$, the surface roughness of rock joints can be measured by the roughness metric $\theta^*_{max}/(C+1)$ [33]. A_0 varies significantly in different directions; thus, the 3D roughness metric A_0 and $\theta^*_{max}/(C+1)$ are both included to fully describe the roughness anisotropy. The 3D morphology parameters of the granite joints, namely, A_0, θ^*_{max}, and C, were calculated using the measured data from 36 surfaces on the basis of equation (6). The values of A_0 and $\theta^*_{max}/(C+1)$ are listed in Table 3. Figure 3 shows the fitting curves of SJ3, SJ12, SJ21, and SJ36 for calculating the roughness parameter C.

Joint wall compressive strength (JCS) is commonly used for representing the influence of rock material strength on the shear behavior of rock joints [3, 8, 25, 39–41]. For the fresh rock, JCS can be replaced by the uniaxial compressive strength σ_c. Based on experimental observation and numerical simulations, several researchers have also found that the failure of asperities in rock joints under direct shear loading was possibly attributed to shear-induced tensile fracture [5, 6, 42–44]. However, the failure mechanism of asperities has not been clearly stated, and controversies still exist. Therefore, uniaxial compressive strength σ_c and tensile strength σ_t of the rock are both selected in this study to describe the effect of rock material strength on the peak shear strength of rock joints.

Basic friction angle φ_b is crucial to determine the shear strength of rock joints. Barton suggested a fundamental form of joint shear strength [3]:

$$\tau_p = \sigma_n \tan[\varphi_b + d_n + s_n], \quad (7)$$

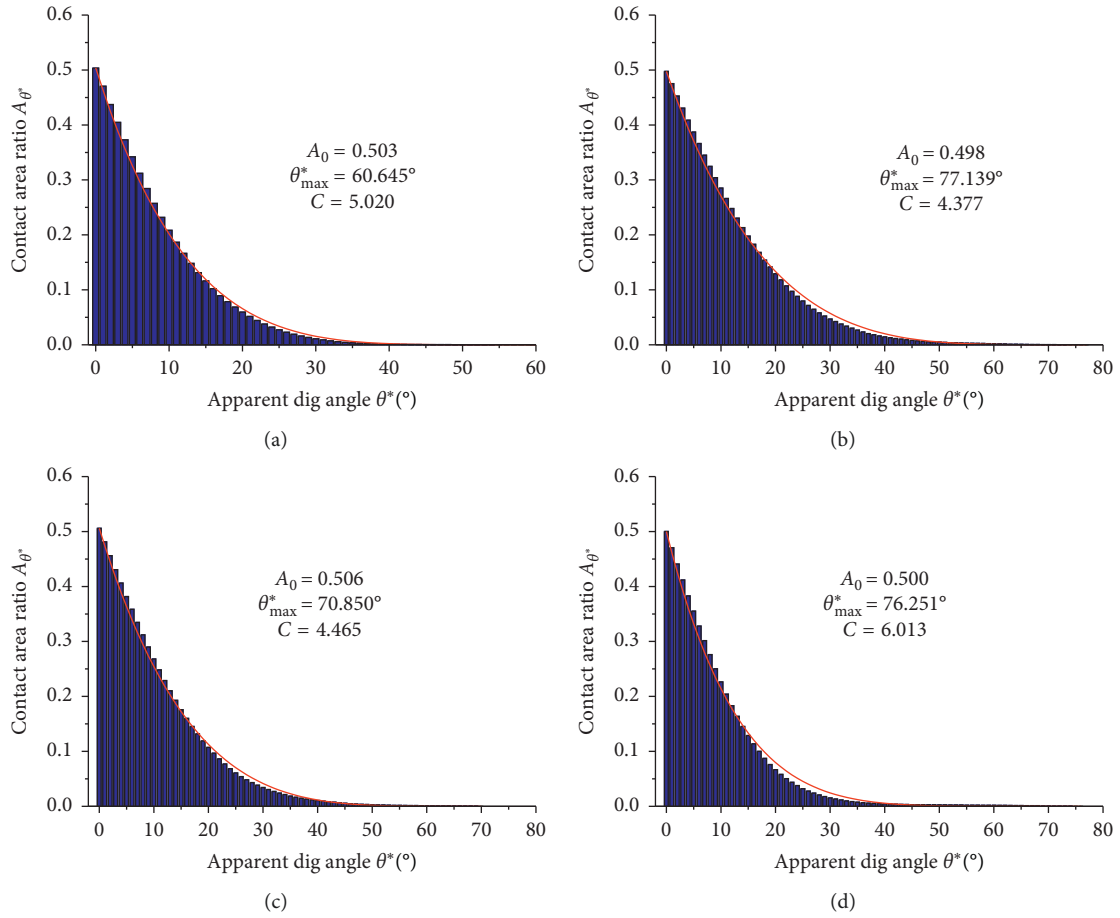

Figure 3: Fitting results of the contact area ratio and apparent dip angle by equation (6): (a) SJ3, (b) SJ12, (c) SJ21, and (d) SJ30.

where σ_n is the normal stress, d_n is the peak dilation angle, and s_n is the shear component angle. On the basis of equation (7), various 2D or 3D morphology parameters have been used for representing the sum of peak dilation angle d_n and shear component angle s_n. No uniform approach for obtaining the basic angle φ_b is currently available. In this work, laboratory direct shear testing method for two smooth joint surfaces is adopted to obtain the basic angle φ_b and the extensive shear strength model, as shown in Table 1.

4.2. Training and Testing of the RVM Model. In this study, the aforementioned original influencing factors, namely, σ_n, σ_c, and σ_t, can be dimensionless preprocessed as two factors: JCS/σ_n and σ_n/σ_t. Therefore, the five influencing factors, which include JCS/σ_n, σ_n/σ_t, A_0, $\theta^*_{max}/(C+1)$, and φ_b, form the input vector of the regression model. All these index values can be measured in the laboratory (see Tables 1–3). Mapping the above five influencing factors to the five-dimensional feature space according to the definition of RVM, the appropriate kernel function was chosen to simplify the nonlinear transformation. The linear kernel function was first used due to its parameter-free and rapid calculation as follows:

$$K(x,z) = \langle x,z\rangle, \tag{8}$$

where $\langle x,z\rangle$ are the training dataset of five influencing factors. The results of direct shear tests on 36 rocks in this study were used to cultivate and advance the RVM model. The results of direct shear tests by Grasselli and Egger [5] and Yang et al. [8] were used for testing the RVM model, in which a total of 50 tests were conducted on five different material types of rock joints (granite, sandstone, limestone, marble, and serpentinite). The 3D morphology parameters of 50 groups of rock joints are represented in Table 4. After the analysis was completed, the quality of the regression model was estimated by the average error formula and correlation coefficient [45]:

$$\overline{\sigma}_{avg} = \frac{1}{n}\sum_{i=1}^{n}\left|\frac{\tau_{mea}-\tau_{est}}{\tau_{mea}}\right| \times 100\%, \tag{9}$$

$$\text{Fitness\_}\overline{\sigma}_{avg} = \frac{\text{train\_}\overline{\sigma}_{avg}\cdot \text{train\_}n + \text{test\_}\overline{\sigma}_{avg}\cdot \text{test\_}n}{\text{train\_}n + \text{test\_}n}, \tag{10}$$

$$R^2 = 1 - \frac{\sum_{i=1}^{n}\left(\tau_{est}-\tau_{mea}\right)^2}{\sum_{i=1}^{n}\left(\tau_{est}-\overline{\tau_{mea}}\right)^2}, \tag{11}$$

$$\text{Fitness\_}R^2 = \frac{\text{train\_}R^2\cdot \text{train\_}n + \text{test\_}R^2\cdot \text{test\_}n}{\text{train\_}n + \text{test\_}n}, \tag{12}$$

Table 4: Comparison between the measured peak shear strength and the calculated results by three different models.

Sample name	JCS/σ_n	σ_n/σ_t	$\theta^*_{max}/(C+1)$ (deg)	A_0	φ_b(deg)	Peak shear strength (MPa)			
						Measured	Grasselli	Yang	Proposed
G1	81.2	0.26	11.016	0.493	34	5.7	4.6	6.0	4.8
G2	81.2	0.26	12.121	0.498	34	5.6	5.1	6.0	4.8
G4	85.2	0.25	10.031	0.498	34	4.8	4.3	4.3	4.6
G5	166.7	0.13	9.005	0.46	34	2.4	2.3	2.0	2.7
G6	166.7	0.13	10.012	0.477	34	2.9	2.4	2.7	2.7
G7	166.7	0.13	9.939	0.47	34	2.8	2.4	2.6	2.7
G9	166.7	0.13	10.949	0.508	34	3.0	2.6	2.6	2.7
C1	23.3	0.45	9.963	0.491	36	2.2	1.9	2.2	1.7
C2	23.3	0.45	12.048	0.462	36	2.1	2.2	2.6	1.8
C3	6.7	1.55	10.179	0.46	36	5.5	5.5	5.1	4.8
C4	10.2	1.02	11.324	0.508	36	4.6	4.1	4.2	3.3
C5	8.1	1.30	11.821	0.495	36	5.0	5.2	5.1	4.1
C6	24.4	0.43	10.985	0.546	36	2.1	2.1	2.1	1.7
C8	8.1	1.30	11.028	0.555	36	4.9	4.9	4.8	4.1
M1	100.0	0.09	7.143	0.513	37	1.7	1.8	1.7	2.1
M2	50.0	0.19	5.909	0.492	37	2.3	3.2	2.4	3.8
M3	100.0	0.09	5.652	0.471	37	1.2	1.7	1.4	2.1
M4	23.3	0.41	6.689	0.513	37	5.8	6.3	5.7	6.3
M5	33.3	0.28	5.948	0.533	37	4.4	4.6	3.8	4.9
M6	33.3	0.28	6.082	0.45	37	4.3	4.4	4.0	4.9
M7	23.3	0.41	6.001	0.502	37	5.6	6.1	5.8	6.2
M8	22.7	0.42	6.250	0.459	37	6.4	6.1	5.7	6.3
M9	33.3	0.28	5.194	0.494	37	4.5	4.4	3.6	4.9
M10	100.0	0.09	5.683	0.515	37	1.5	1.7	1.4	2.1
M12	47.6	0.09	6.643	0.429	37	3.0	3.6	2.8	3.8
ML1	9.8	1.46	8.000	0.573	37	1.4	1.3	1.4	1.4
ML2	2.4	5.90	6.988	0.505	37	4.5	4.8	3.7	5.1
ML3	4.8	2.99	7.491	0.523	37	2.3	4.7	2.2	2.7
S1	83.3	0.32	13.621	0.504	39	4.3	6.0	8.1	5.2
S2	166.7	0.16	13.787	0.466	39	3.4	1.9	4.1	3.1
Granite (G3)	201.3	0.09	7.075	0.61	34	1.5	1.5	1.5	1.3
Granite (G4)	100.6	0.18	7.535	0.53	34	3.1	2.9	3.0	3.4
Granite (G5)	67.1	0.27	7.551	0.48	34	4.8	4.0	4.4	4.9
Granite (G6)	50.3	0.36	7.982	0.51	34	5.8	5.2	5.8	6.1
Granite (G7)	40.3	0.45	6.952	0.47	34	6.4	5.8	6.4	7.1
Granite (G8)	33.5	0.55	6.902	0.49	34	7.3	6.7	7.5	7.9
Granite (G9)	28.8	0.64	6.661	0.53	34	8.5	7.6	8.3	8.7
Granite (G10)	25.2	0.73	7.959	0.56	34	11.0	8.8	10.5	9.6
Granite (G11)	22.4	0.82	7.784	0.51	34	11.2	9.3	11.2	10.4
Granite (G12)	20.1	0.91	8.842	0.53	34	12.7	10.6	13.3	11.2
Sandstone (S3)	200.0	0.13	8.459	0.51	28	0.7	0.5	0.5	0.4
Sandstone (S4)	100.0	0.25	9.555	0.61	28	0.9	1.0	1.1	1.1
Sandstone (S5)	66.7	0.38	8.797	0.54	28	1.5	1.3	1.5	1.6
Sandstone (S6)	50.0	0.50	8.453	0.49	28	2.0	1.6	1.9	2.0
Sandstone (S7)	40.0	0.63	7.863	0.55	28	2.1	1.9	2.3	2.3
Sandstone (S8)	33.3	0.75	9.150	0.58	28	3.0	2.3	2.9	2.6
Sandstone (S9)	28.6	0.88	8.344	0.5	28	3.3	2.4	3.1	2.9
Sandstone (S10)	25.0	1.00	8.489	0.47	28	3.6	2.6	3.5	3.2
Sandstone (S11)	22.2	1.13	8.116	0.44	28	3.8	2.8	3.8	3.5
Sandstone (S12)	20.0	1.25	9.016	0.51	28	4.7	3.3	4.4	3.7

where $\overline{\sigma}_{avg}$ is the average estimation error, n is the sample size, τ_{mea} is the measured peak shear strength, τ_{est} is the estimated peak shear strength, $\overline{\tau_{mea}}$ is the average value of the measured peak shear strength, Fitness_$\overline{\sigma}_{avg}$ is the comprehensive estimation error of the RVM model, and Fitness_R^2 is the correlation coefficient of the train and test model; train_n is the number of the training sample, and test_n is the number of the testing sample. In this work, train_n and test_n are 36 and 50, respectively. The average estimation errors of the RVM model for the training and testing data are 6.46% and 21.12%, respectively. The correlation coefficient of the RVM model for the training and testing data is 0.977 and 0.769, respectively. The comprehensive estimation error Fitness_$\overline{\sigma}_{avg}$ and correlation coefficient Fitness_R^2 of the

RVM model for all the data are 14.98% and 0.856, respectively. This finding indicates that the RVM model exhibits good training accuracy and high generalization capacity. Therefore, the RVM model is feasible and effective for estimating the peak shear strength of rock joints and can be used in practical applications.

5. Comparison and Discussion

5.1. RVM with Different Kernel Functions. The inner product of kernel functions is usually substituted for the complex calculation of high-dimensional feature space to deal with the dimensionality problem under high-dimensional feature space. The nonlinear shining mode from the raw feature space to high-dimensional space relays on the type of kernel functions. The approximate kernel function and model parameters have a considerable effect on the model stability and regression precision [46].

To further enhance the accuracy of the proposed model, three other common kernel functions were introduced: polynomial kernel function, Gaussian kernel function, and sigmoid kernel function.

$$\text{Polynomial kernel function: } K(x,z) = (a \cdot \langle x,z\rangle + b)^c, \tag{13}$$

$$\text{Gaussian kernel function: } K(x,z) = \exp\left(\frac{-\|x-z\|^2}{2d^2}\right), \tag{14}$$

$$\text{Sigmoid kernel function: } K(x,z) = \tanh(k \cdot \langle x,z\rangle + p), \tag{15}$$

Table 5: Kernel function parameters and average estimation errors.

Kernel function type	Fitness_$\overline{\sigma}_{avg}$ (%)	Fitness_R^2	Parameter number
Linear	14.98	0.856	0
Polynomial	12.41	0.957	3
Gaussian	12.24	0.956	1
Sigmoid	13.44	0.952	2

where a, b, c, d, k, and p are kernel function parameters.

In the RVM model, the kernel function parameters must be defined. The most relevant papers which include the determination of the optimal kernel function parameters for RVM is lacking. Several different values of kernel function parameters were selected as determining which one provides better regression accuracy. The four kernel function parameters and the accompanying average estimation errors and correlation coefficients are represented in Table 5. Synthetically considering the regression performance and the kernel function parameter number, a peak shear strength of RVM model based on a Gaussian kernel function is established. The optimal value of the kernel function parameter d is 52.43.

5.2. Comparison with Existing Criteria. To certify the rationality of the proposed model, the two models developed by Grasselli and Egger [5] and Yang et al. [8] have been chosen for comparison.

$$\text{Grasselli's model: } \tau_p = \left[1 + \exp\left(-\frac{\theta^*_{\max}\sigma_n}{9A_0C\sigma_t}\right)\right]\sigma_n \tan\left[\varphi_b + \left(\frac{\theta^*_{\max}}{C}\right)^{1.18\cos\beta}\right], \tag{16}$$

$$\text{Yang's model: } \tau_p = \sigma_n \tan\left[\varphi_b + \frac{\theta^*_{\max}}{C^{0.45}} e^{(-\sigma_n/\mathrm{JCS})C^{0.75}}\right]. \tag{17}$$

The 3D morphology parameters of the 50 rock joints are represented in Table 4. The estimated results using equations (16) and (17), the RVM model results, and the measured peak shear strength are listed in Table 4. The prediction results of the peak shear strength of rock joints are compared with the measured data, as shown in Figures 4 and 5.

According to equation (9), the mean errors of the estimated value results calculated using Grasselli's model, Yang's model, and RVM model are 16.3%, 8.9%, and 15.4%, respectively. Based on equation (11), the correlation values of the estimated value results calculated using Grasselli's model, Yang's model, and RVM model are 0.889, 0.940, and 0.938, respectively. From the mean error and correlation coefficient analysis, the average estimation error values of the three models are less than 20% and the correlation coefficients are greater than 0.85, which indicate that the three models were quite efficient to be used to predict the shear strength of rock joints. Moreover, the proposed model is more accurate than that of Grasselli's model and has almost equivalent precision to that of Yang's model. After analysis of the above average errors, the existent limitations of the three models should be pointed out. In Grasselli's and Yang's models, the function forms are complex. According to Grasselli's model (i.e., equation (14)), the ratio ($\theta^*_{\max}/C$) was taken as a measure of joint surface roughness, but C cannot be zero ($C = 0$ for saw-tooth joints). Yang's model is not fully explained on how to use the two parameters $\theta^*_{\max}$ and C in combination, and A_0 is not even considered. Furthermore, Grasselli and Egger [5] and Yang et al. [8] deemed that the actual contact area was closely related with

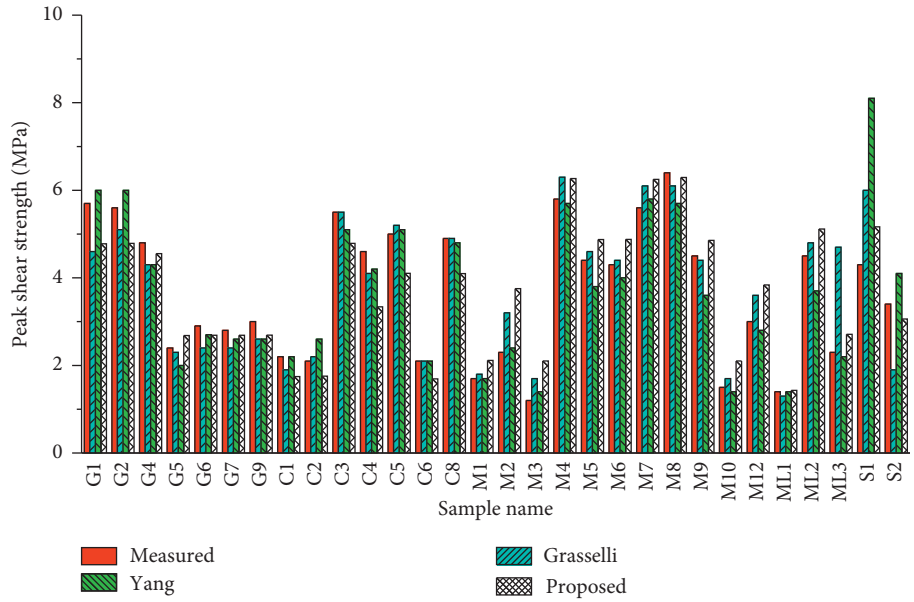

FIGURE 4: Measured peak shear strength of rock joints by Grasselli and Egger [5], which was calculated using Grasselli's model, Yang's model, and the proposed model.

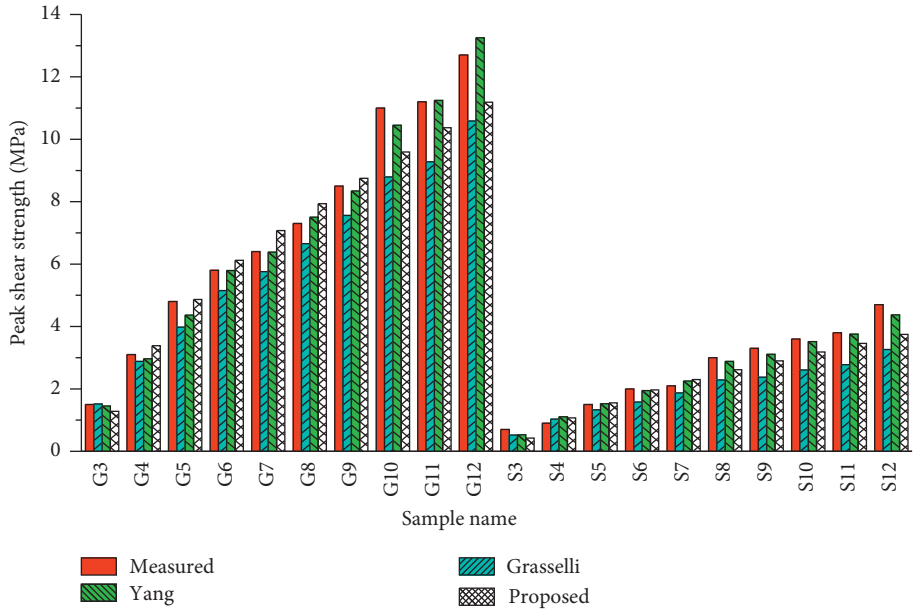

FIGURE 5: Measured peak shear strength of rock joints by Yang et al. [8], which was calculated using Grasselli's model, Yang's model, and the proposed model.

σ_n/σ_t and σ_n/σ_c, respectively. Compared with Grasselli's and Yang's models, the proposed model was less complex for large samples and comprehensively considered many factors; in particular, the effect of compressive strength and tensile strength on the peak shear strength of rock joints was first investigated. However, the determination of kernel function parameter needs to be further improved and optimized.

In this study, the investigation is limited to the shear behavior of unfilled joints. Influencing factors, such as size of joint (scale effect), sampling interval, joint matching coefficient, and joint filling, should be further investigated. Although the proposed model has limitations, it is believed to be a novel research idea for assessing peak shear strength of rock joints.

6. Conclusions

The hybrid probabilistic regression assessment algorithm RVM was accustomed to identify the peak shear strength of the rock joint, with Gaussian kernel function being introduced to improve the prediction accuracy. The direct

shear tests on joint specimens were conducted to train the new model, and its rationality on assessing the peak shear strength was also validated. Some concluding remarks are presented as follows:

(1) A novel intelligent peak shear strength model combined with RVM was supposed to assess the peak shear strength of rock joints, which can comprehensively consider the elements influencing the peak shear strength, such as normal stress, joint surface roughness, rock strength, and basic friction angle. The 36 natural granite joint specimens were accustomed to examine the suggested model, and the result reflects that the RVM model exhibits good training accuracy and high generalization capacity.

(2) Four types of kernel functions were investigated for their performance in regression accuracy in the RVM model. According to the regression performance and the kernel function parameter number, the Gaussian kernel function was determined to be the better one combined with the RVM model. The optimal value of the kernel function parameter d is 52.43.

(3) The peak shear model of Grasselli's and Yang's was chosen for comparison with the proposed model. Based on the 3D morphology parameters of 50 rock joints, the prediction results show that the proposed model can meet the accuracy requirements. In addition, the new model has less complexity and can take into account the effects of compressive strength and tensile strength on the peak shear strength of rock joints.

Data Availability

The data used to support the findings of this study are included within the article.

Conflicts of Interest

The authors declare no conflicts of interest.

Acknowledgments

The study was funded by the Natural Science Foundation of Zhejiang Province (no. LY18D020003) and the National Natural Science Foundation of China (nos. 41327001, 41572299, 41427802). This support was gratefully acknowledged.

Supplementary Materials

1. The file named topograph_3D is the code for the 3D parameter of $\theta^*_{\max}/(C+1)$. 2. The file named Data contains two sheets, one of which is the prediction of the shear strength, and the second is the comparison of the kernel functions. 3. The file named 3D roughness parameter is the fitting curves of SJ3, SJ12, SJ21, and SJ30 for calculating the roughness parameter C. 4. The file named Comparation is the display of the shear strength prediction comparison with the model of Grasselli's and Yang's. (*Supplementary Materials*)

References

[1] D. Huang, C. Yang, B. Zeng, and G. Fu, "A copula-based method for estimating shear strength parameters of rock mass," *Mathematical Problems in Engineering*, vol. 2014, Article ID 693062, 11 pages, 2014.

[2] F. D. Patton, "Multiple modes of shear failure in rock," in *Proceedings of 1st Congress of International Society for Rock Mechanics*, pp. 509–513, Lisbon, Portugal, October 1966.

[3] N. Barton, "Review of a new shear-strength criterion for rock joints," *Engineering Geology*, vol. 7, no. 4, pp. 287–332, 1973.

[4] P. H. S. W. Kulatilake, G. Shou, T. H. Huang, and R. M. Morgan, "New peak shear strength criteria for anisotropic rock joints," *International Journal of Rock Mechanics and Mining Sciences & Geomechanics Abstracts*, vol. 32, no. 7, pp. 673–697, 1995.

[5] G. Grasselli and P. Egger, "Constitutive law for the shear strength of rock joints based on three-dimensional surface parameters," *International Journal of Rock Mechanics and Mining Sciences*, vol. 40, no. 1, pp. 25–40, 2003.

[6] C.-C. Xia, Z.-C. Tang, W.-M. Xiao, and Y.-L. Song, "New peak shear strength criterion of rock joints based on quantified surface description," *Rock Mechanics and Rock Engineering*, vol. 47, no. 2, pp. 387–400, 2014.

[7] Z. C. Tang and L. N. Y. Wong, "New criterion for evaluating the peak shear strength of rock joints under different contact states," *Rock Mechanics and Rock Engineering*, vol. 49, no. 4, pp. 1191–1199, 2016.

[8] J. Yang, G. Rong, D. Hou, J. Peng, and C. Zhou, "Experimental study on peak shear strength criterion for rock joints," *Rock Mechanics and Rock Engineering*, vol. 49, no. 3, pp. 821–835, 2016.

[9] C. C. Garcia-Fernandez, C. Gonzalez-Nicieza, M. I. Alvarez-Fernandez, and R. A. Gutierrez-Moizant, "New methodology for estimating the shear strength of layering in slate by using the Brazilian test," *Bulletin of Engineering Geology and the Environment*, vol. 78, no. 4, pp. 2283–2297, 2019.

[10] J. P. Seidel and C. M. Haberfield, "The application of energy principles to the determination of the sliding resistance of rock joints," *Rock Mechanics and Rock Engineering*, vol. 28, no. 4, pp. 221–226, 1995.

[11] F. Lanaro and O. Stephansson, "A unified model for characterisation and mechanical behaviour of rock fractures," *Thermo-Hydro-Mechanical Coupling in Fractured Rock*, vol. 160, no. 5-6, pp. 989–998, 2003.

[12] Z. C. Tang, Y. Y. Jiao, L. N. Y. Wong, and X. C. Wang, "Choosing appropriate parameters for developing empirical shear strength criterion of rock joint: review and new insights," *Rock Mechanics and Rock Engineering*, vol. 49, no. 11, pp. 4479–4490, 2016.

[13] J. Ye, R. Yong, Q.-F. Liang, M. Huang, and S.-G. Du, "Neutrosophic functions of the joint roughness coefficient and the shear strength: a case study from the pyroclastic rock mass in Shaoxing city, China," *Mathematical Problems in Engineering*, vol. 2016, Article ID 4825709, 9 pages, 2016.

[14] H. Lin, S. Xie, R. Yong, Y. Chen, and S. Du, "An empirical statistical constitutive relationship for rock joint shearing considering scale effect," *Comptes Rendus Mécanique*, vol. 347, no. 8, pp. 561–575, 2019.

[15] H. Lin, H. Yang, Y. Wang, Y. Zhao, and R. Cao, "Determination of the stress field and crack initiation angle of an

open flaw tip under uniaxial compression," *Theoretical and Applied Fracture Mechanics*, vol. 104, Article ID 102358, 2019.

[16] I. Yilmaz and A. Yuksek, "An example of artificial neural network (ANN) application for indirect estimation of rock parameters," *Rock Mechanics and Rock Engineering*, vol. 41, no. 5, pp. 781–795, 2008.

[17] K. Sarkar, A. Tiwary, and T. N. Singh, "Estimation of strength parameters of rock using artificial neural networks," *Bulletin of Engineering Geology and the Environment*, vol. 69, no. 4, pp. 599–606, 2010.

[18] N. Ceryan, U. Okkan, and A. Kesimal, "Prediction of unconfined compressive strength of carbonate rocks using artificial neural networks," *Environmental Earth Sciences*, vol. 68, no. 3, pp. 807–819, 2013.

[19] E. Momeni, D. Jahed Armaghani, M. Hajihassani, and M. F. Mohd Amin, "Prediction of uniaxial compressive strength of rock samples using hybrid particle swarm optimization-based artificial neural networks," *Measurement*, vol. 60, pp. 50–63, 2015.

[20] D. J. Armaghani, E. T. Mohamad, E. Momeni, M. Monjezi, and M. S. Narayanasamy, "Prediction of the strength and elasticity modulus of granite through an expert artificial neural network," *Arabian Journal of Geosciences*, vol. 9, no. 1, p. 48, 2016.

[21] L. K. Sharma, V. Vishal, and T. N. Singh, "Developing novel models using neural networks and fuzzy systems for the prediction of strength of rocks from key geomechanical properties," *Measurement*, vol. 102, pp. 158–169, 2017.

[22] V. N. Vapnik, *Statistical Learning Theory*, Wiley, New York, NY, USA, 1998.

[23] D. Park and L. R. Rilett, "Forecasting freeway link travel times with a multilayer feed forward neural network," *Computer-Aided Civil and Infrastructure Engineering Journal*, vol. 14, no. 5, pp. 357–367, 1999.

[24] P. Samui, T. Lansivaara, and D. Kim, "Utilization relevance vector machine for slope reliability analysis," *Applied Soft Computing*, vol. 11, no. 5, pp. 4036–4040, 2011.

[25] M. Marjanović, M. Kovačević, B. Bajat, and V. Voženílek, "Landslide susceptibility assessment using SVM machine learning algorithm," *Engineering Geology*, vol. 123, no. 3, pp. 225–234, 2011.

[26] X. Qian, J. Chen, L.-J. Xiang, L. Xiang, W. Zhang, and C. Niu, "A novel hybrid KPCA and SVM with PSO model for identifying debris flow hazard degree: a case study in Southwest China," *Environmental Earth Sciences*, vol. 75, no. 11, p. 991, 2016.

[27] R. Gholami, V. Rasouli, and A. Alimoradi, "Improved RMR rock mass classification using artificial intelligence algorithms," *Rock Mechanics and Rock Engineering*, vol. 46, no. 5, pp. 1199–1209, 2013.

[28] M. E. Tipping, "Sparse Bayesian learning and the relevance vector machine," *Journal of Machine Learning Research*, vol. 1, pp. 1211–1244, 2001.

[29] M. E. Tipping, "Bayesian inference: an introduction to principles and practice in machine learning," in *Advanced Lectures on Machine Learning*, pp. 41–46, Springer, Berlin, Germany, 2004.

[30] P. Samui and B. Dixon, "Application of support vector machine and relevance vector machine to determine evaporative losses in reservoirs," *Hydrological Processes*, vol. 26, no. 9, pp. 1361–1369, 2012.

[31] W. Hatheway, "The complete ISRM suggested methods for rock characterization, testing and monitoring: 1974–2006," *Environmental and Engineering Geoscience*, vol. 15, no. 1, pp. 47-48, 2009.

[32] C. C. Xia, X. Qian, P. Lin, W. M. Xiao, and Y. Gui, "Experimental investigation of nonlinear flow characteristics of real rock joints under different contact conditions," *Journal of Hydraulic Engineering*, vol. 143, no. 3, Article ID 04016090, 2017.

[33] B. S. A. Tatone and G. Grasselli, "A method to evaluate the three-dimensional roughness of fracture surfaces in brittle geomaterials," *Review of Scientific Instruments*, vol. 80, no. 12, Article ID 125110, 2009.

[34] N. Barton and V. Choubey, "The shear strength of rock joints in theory and practice," *Rock Mechanics Felsmechanik Mecanique des Roches*, vol. 10, no. 1-2, pp. 1–54, 1977.

[35] I. W. Yeo, M. H. de Freitas, and R. W. Zimmerman, "Effect of shear displacement on the aperture and permeability of a rock fracture," *International Journal of Rock Mechanics and Mining Sciences*, vol. 35, no. 8, pp. 1051–1070, 1998.

[36] G. Grasselli, "Manuel rocha medal recipient shear strength of rock joints based on quantified surface description," *Rock Mechanics and Rock Engineering*, vol. 39, no. 4, pp. 295–314, 2006.

[37] Z.-C. Tang, Q.-S. Liu, and J.-H. Huang, "New criterion for rock joints based on three-dimensional roughness parameters," *Journal of Central South University*, vol. 21, no. 12, pp. 4653–4659, 2014.

[38] G. Grasselli, J. Wirth, and P. Egger, "Quantitative three-dimensional description of a rough surface and parameter evolution with shearing," *International Journal of Rock Mechanics and Mining Sciences*, vol. 39, no. 6, pp. 789–800, 2002.

[39] S. Saeb and B. Amadei, "Modelling rock joints under shear and normal loading," *International Journal of Rock Mechanics and Mining Sciences & Geomechanics Abstracts*, vol. 29, no. 3, pp. 267–278, 1992.

[40] F. Johansson and H. Stille, "A conceptual model for the peak shear strength of fresh and unweathered rock joints," *International Journal of Rock Mechanics and Mining Sciences*, vol. 69, pp. 31–38, 2014.

[41] Q. Liu, Y. Tian, P. Ji, and H. Ma, "Experimental investigation of the peak shear strength criterion based on three-dimensional surface description," *Rock Mechanics and Rock Engineering*, vol. 51, no. 4, pp. 1005–1025, 2018.

[42] M. S. Asadi, V. Rasouli, and G. Barla, "A laboratory shear cell used for simulation of shear strength and asperity degradation of rough rock fractures," *Rock Mechanics and Rock Engineering*, vol. 46, no. 4, pp. 683–699, 2013.

[43] A. H. Ghazvinian, M. J. Azinfar, and R. Geranmayeh Vaneghi, "Importance of tensile strength on the shear behavior of discontinuities," *Rock Mechanics and Rock Engineering*, vol. 45, no. 3, pp. 349–359, 2012.

[44] Y. Tian, Q. Liu, D. Liu, Y. Kang, P. Deng, and F. He, "Updates to grasselli's peak shear strength model," *Rock Mechanics and Rock Engineering*, vol. 51, no. 7, pp. 2115–2133, 2018.

[45] G. Grasselli, *Shear strength of rock joints based on quantified surface description*, Swiss Federal Institute of Technology, Zurich, Switzerland, Ph.D. dissertation, 2001.

[46] F. Kuang, W. Xu, and S. Zhang, "A novel hybrid KPCA and SVM with GA model for intrusion detection," *Applied Soft Computing*, vol. 18, pp. 178–184, 2014.

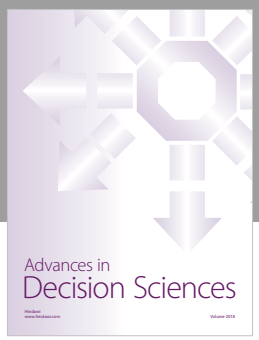

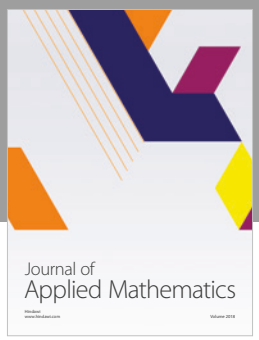

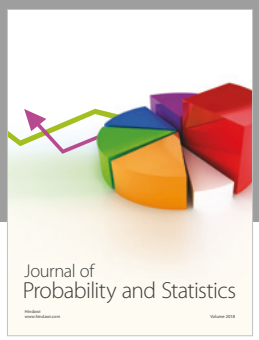

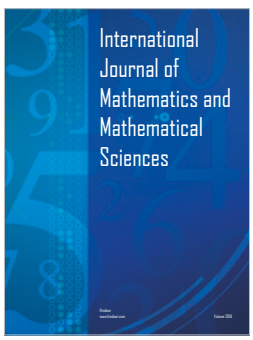

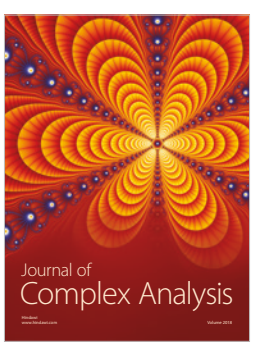

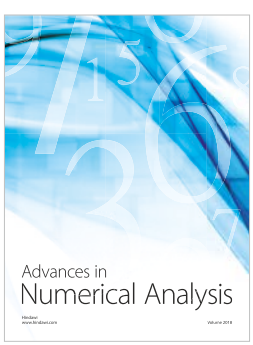

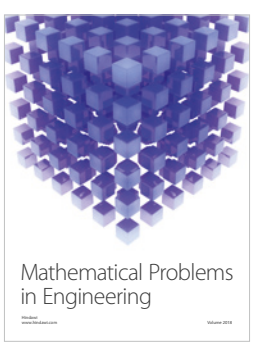

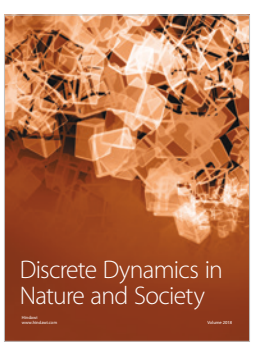

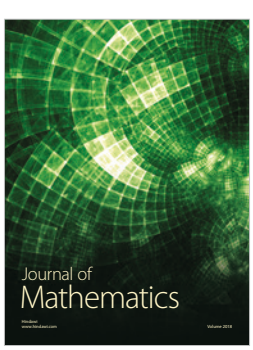

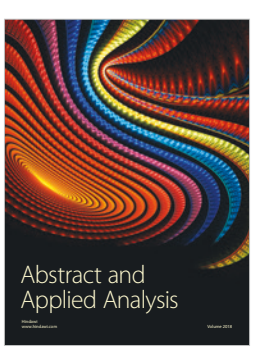

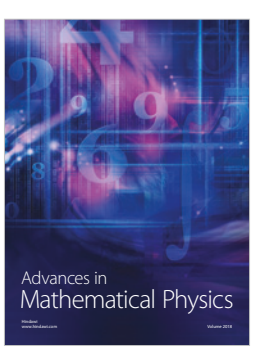

Hindawi

Submit your manuscripts at
www.hindawi.com